Journal of Magnetic Resonance 213 (2011) 22–25

Contents lists available at SciVerse ScienceDirect

Journal of Magnetic Resonance

journal homepage: www.elsevier.com/locate/jmr

Long-lived NMR echoes in solids

A.K. Khitrin

Department of Chemistry, Kent State University, Kent, OH 44242, United States

ARTICLE INFO

Article history:
Received 30 April 2011
Revised 11 August 2011
Available online 23 August 2011

Keywords:
Spin echo
Long-lived
Solids

ABSTRACT

A new type of long-lived NMR echo in solids with homogeneously broadened dipolar spectra is discussed. The echo can be generated by a simple two-pulse Hahn sequence in solid samples, where dipolar-coupled nuclei have different chemical shifts. We present general considerations and simple theoretical models which explain some features of this phenomenon.

1. Introduction

It has been known that, for homogeneously broadened dipolar NMR spectra of solids, weak and long pulses can excite sharp response signals, which are orders of magnitude narrower than the conventional spectra [1–3]. So far, the attempts of explaining this phenomenon have not been very successful. Very recently, it has been found that the underlying mechanism is a new type of long-lived echo, based on broken symmetry [4]. Whenever a single long pulse can produce long free-induction decay (FID) signal, there also exists a long-lived echo, generated by the two-pulse Hahn sequence [5]. This long-lived echo can be found in all homonuclear samples with non-equivalent nuclei (different chemical shifts) coupled by dipole–dipole interactions, as well as in heteronuclear systems. Why this type of long-lived echo, observed in a simple two-pulse experiment, waited so long to be discovered? Probably, each time when such small-amplitude echoes have been observed in experiments, they were misinterpreted as coming from "liquid"-phase contamination. However, many features of the new echo are inconsistent with an explanation by a presence of inhomogeneously broadened signal from "liquid". Besides that, for inhomogeneous broadening, dephasing/refocusing of individual spectral components of magnetization takes place in the x–y plane of the rotating frame. For the echo we discuss, dephasing/refocusing occurs is a more complex space of many-spin operators. This difference can be easily verified in experiments.

The purpose of this paper is to supplement Ref. [4] by providing more explanations, theoretical considerations, and model calculations. In the next section we derive expressions for the signal excited by a soft pulse followed by a hard refocusing pulse. Compared to Ref. [4], the calculation is done in a more explicit and general way, and the result is obtained in a simpler form. Section 3 contains exact calculations for the three-level model, introduced in [4]. We also present some additional qualitative considerations related to the echo amplitude, decay rate, shape, and the role of molecular motions.

Even though not all characteristics of the long-lived echo are well understood at this moment, we feel that the discussion below may be useful. The new type of long-lived NMR echo in solids is a manifestation of complex collective many-spin dynamics. Therefore, explicit models, like the three-level model in Section 3, will be necessarily oversimplified and capable of grasping only few features of the real spin dynamics.

2. Selective echo

We will start by explaining why a soft selective pulse cannot produce slowly decaying magnetization unless there also exists a long-lived echo, excited by a sequence of two hard pulses. In this section, we consider the signal generated by a sequence of a soft (weak and long) y-pulse with the amplitude $f(t)$, followed by a hard refocusing pulse. For simplicity, the soft pulse will be symmetric: $f(t) = f(-t)$, and it will be also assumed that the total flip angle of the soft pulse is small: $\varphi = \int_{-T}^{T} dt\, f(t) \ll 1$, where $2T$ is the pulse duration.

In the first part of this section we reproduce some calculations in Ref. [4] in order to introduce more convenient notations, and also to show the calculations and results in a more explicit way. Suppose that a spin system evolves under the time-independent Hamiltonian H, and both the initial density matrix $\rho(0)$ and the observable are S_X. Then x-component of magnetization $M(t)$, or the free-induction decay (FID) signal, is

$$M(t) = \langle S_X|\rho(t)\rangle = \langle S_X|S_X(t)\rangle, \quad \text{where } |S_X(t)\rangle = \exp(L_H t)|S_X\rangle. \qquad (1)$$

E-mail address: akhitrin@kent.edu

1090-7807/$ - see front matter © 2011 Elsevier Inc. All rights reserved.
doi:10.1016/j.jmr.2011.08.024

Here $L_H = -i[H, \ldots]$ is the Liouvillian, the binary product for the two operators A and B is defined as $\langle A|B\rangle = Tr(A^+B)$, and A^+ is the Hermitian conjugate of A. We will also use normalization $\langle S_X|S_X\rangle = 1$, so that the FID signal in Eq. (1) is normalized. It is convenient to introduce the spectral components $|\omega\rangle$ of the operator $|S_X(t)\rangle$ as

$$|\omega\rangle = \int dt \exp(-i\omega t)|S_X(t)\rangle, \qquad |S_X(t)\rangle = \int d\omega \exp(i\omega t)|\omega\rangle. \quad (2)$$

Here and below the integration symbol without limits means integration between $-\infty$ and ∞.

Now let us assume that the equilibrium density matrix is S_Z and the signal is created by a soft y-pulse with the amplitude $f(t)$ and small total flip angle. The linear-response density matrix created by the pulse at time $t = T$ is

$$|\rho(T)\rangle = \int d\omega \int_{-T}^{T} dt f(t) \exp(i\omega(T-t))|\omega\rangle, \quad (3)$$

i.e. each spectral component of the linear response, created at time t with the rate $f(t)$, has evolved during time $T-t$ after its creation. Since $f(t) = 0$ at $|t| > T$, the integration limits in (3) can be omitted:

$$\begin{aligned}|\rho(T)\rangle &= \int d\omega \exp(i\omega T) \int dt f(t) \exp(-i\omega t)|\omega\rangle \\ &= \int d\omega \exp(i\omega T) f(\omega)|\omega\rangle, \end{aligned} \quad (4)$$

where $f(\omega)$ is the Fourier transform of $f(t)$. The phase factors in Eq. (4) are the same as resulting from δ-excitation at $t = 0$ (compare to Eq. (2)), but the excitation profile is "tailored" by the function $f(\omega)$. It is easy to see that, without the refocusing pulse at $t = T$, the signal is zero at $t > T$ if the spectral width of $f(\omega)$ is much narrower than that of the conventional spectrum:

$$\begin{aligned} M(t>T) = \langle S_X|\rho(t)\rangle &= \int d\omega_1 d\omega exp(i\omega t) f(\omega)\langle\omega_1|\omega\rangle \\ &= \int d\omega I_0(\omega) \exp(i\omega t) f(\omega) \approx I_0(0) \int d\omega \exp(i\omega t) f(\omega) \\ &= I_0(0) f(t) = 0. \end{aligned} \quad (5)$$

Here the projector $\langle\omega_1|\omega\rangle = \delta(\omega_1 - \omega)\ I_0(\omega_1)$ can be calculated directly from Eqs. (1) and (2), and $I_0(\omega)$ is the conventional line shape.

Let us suppose that after the soft excitation pulse, at the moment $t = T$, the Hamiltonian changes from H to H', and the subsequent evolution happens with the Hamiltonian H'. Similar to the spectral components $|\omega\rangle$, we can introduce the operator S'_X and its spectral components $|\omega'\rangle$ for the Hamiltonian H'. Magnetization at time $t > T$ is contributed only by the operators $|\omega'\rangle$. Projection of the density matrix on this subspace at $t = T$ can be represented as

$$|\rho'(T)\rangle = \int d\omega'' a(\omega'', T)|\omega''\rangle, \quad (6)$$

where $a(\omega'',T)$ are numerical coefficients. The coefficients $a(\omega'',T)$ can be calculated from equal projections of $|\rho\rangle$ and $|\rho'\rangle$ on the subspace $|\omega'\rangle$:

$$\begin{aligned}\langle\omega'|\rho(T)\rangle = \langle\omega'|\rho'(T)\rangle &= \int d\omega'' a(\omega'', T)\langle\omega'|\omega''\rangle \\ &= \int d\omega'' \delta(\omega' - \omega'') I'_0(\omega') a(\omega'', T) = I'_0(\omega') a(\omega', T). \end{aligned} \quad (7)$$

Therefore, the coefficients are

$$a(\omega', T) = \langle\omega'|\rho(T)\rangle (I'_0(\omega'))^{-1}. \quad (8)$$

By inserting the density matrix $|\rho(T)\rangle$ from Eq. (4) into Eq. (8), and using Eq. (6), one can now calculate the signal at $t > T$:

$$\begin{aligned} M(t>T) &= \int d\omega' d\omega'' \langle\omega''| \exp(i\omega'(t-T)) a(\omega', T)|\omega'\rangle \\ &= \int d\omega' d\omega'' \langle\omega''| \exp(i\omega'(t-T))|\omega'\rangle\langle\omega'|\rho(T)\rangle (I'_0(\omega'))^{-1} \\ &= \int d\omega' d\omega'' \langle\omega''| \exp(i\omega'(t-T))|\omega'\rangle\langle\omega'| \\ &\quad \times \int d\omega \exp(i\omega T) f(\omega)|\omega\rangle (I'_0(\omega'))^{-1} \\ &= \int d\omega d\omega' \exp(i\omega'(t-T)) \exp(i\omega T) f(\omega)\langle\omega'|\omega\rangle. \end{aligned} \quad (9)$$

In Eqs. (7)–(9) we used for the "new" operators $\langle\omega''|\omega'\rangle = \delta(\omega'' - \omega') I'_0(\omega'')$, where $I'_0(\omega)$ is the conventional line shape with the Hamiltonian H'. The projections $\langle\omega'|\omega\rangle$ of "new" operators on "old" operators in Eq. (9) can be calculated by using their definition in Eqs. (2) and (1):

$$\langle\omega'|\omega\rangle = \int d\tau' d\tau \exp(i\omega'\tau') \exp(-i\omega\tau)\langle S'_X(\tau')|S_X(\tau)\rangle, \quad (10)$$

where the time dependence of $|S'_X(\tau)\rangle$ is defined by the Hamiltonian H'. Since the operators $|\exp(L_H t) S_X\rangle$ in Eq. (1) are Hermitian, the transformation from "ket" to "bra" operators requires only a complex conjugation for the phase factors $\exp(-i\omega t)$. Then, by substituting Eq. (10) into Eq. (9) and integrating over ω and ω', one obtains

$$\begin{aligned} M(t>T) &= \int d\omega' d\omega \exp(i\omega'(t-T)) \exp(i\omega T) f(\omega) \\ &\quad \times \int d\tau' d\tau \exp(i\omega'\tau') \exp(-i\omega\tau)\langle S'_X(\tau')|S_X(\tau)\rangle \\ &= \int d\tau' d\tau \delta(\tau' + t - T) f(T-\tau)\langle S'_X(\tau')|S_X(\tau)\rangle \\ &= \int d\tau f(T-\tau)\langle S'_X(T-t)|S_X(\tau)\rangle. \end{aligned} \quad (11)$$

This simple equation in time domain could be written directly by using the same reasoning as we did to introduce Eq. (3). The purpose of switching to frequency domain and then back to time domain was to learn several things on the way. First, a long weak pulse selects spectral components with arbitrarily narrow spectral range (Eq. (4)), and the created long-lived state is far from equilibrium. Second, the spectral components are perfectly dephased (Eq. (5)) and, therefore, no linear response signal can be observed. This is true for arbitrary pulse shape and the system's Hamiltonian (including also the systems with inhomogeneous broadening). Third, sudden change of the Hamiltonian does not do any magic in refocusing these spectral components unless there exists an echo for a sequence of two hard pulses (see below).

There are two simple cases of Eq. (11):

(1) $H' = H$. In this case $\langle S'_X(T-t)|S_X(\tau)\rangle = M_0(T-t-\tau) = M_0(t-T+\tau)$, and Eq. (11) becomes

$$M(t>T) = \int d\tau f(T-\tau) M_0(t-T+\tau) \approx I_0(0) f(t) = 0. \quad (12)$$

Eq. (12) is an expected summation of free induction signals, created at earlier moments of time. There is no echo signal.

(2) $H' = -H$. In this case $\langle S'_X(T-t)|S_X(\tau)\rangle = M_0(-T+t-\tau)$, and Eq. (11) becomes

$$M(t>T) = \int d\tau f(T-\tau) M_0(-T+t-\tau) \approx I_0(0) f(2T-t), \quad (13)$$

describing an ideally refocused echo at $T < t < 3T$, which replicates the (time-reversed) excitation profile $f(t)$.

In general, Eq. (11) shows that a long-lived echo, centered at $t = 2T$, can exist only when the correlator $\langle S'_X(T-t)|S_X(\tau)\rangle$ has a long-lived component at $t = T + \tau$:

$$\langle S'_X(-\tau)|S_X(\tau)\rangle = \langle \exp(-L_{H'}\tau)S_X|\exp(L_H\tau)S_X\rangle = \langle S_X|\exp(L_{H'}\tau)\exp(L_H\tau)S_X\rangle. \quad (14)$$

Eq. (14) is exactly the echo amplitude at $t = 2\tau$ for non-selective excitation, when the signal is created at $t = 0$, and the refocusing pulse is applied at $t = \tau$. Therefore, the soft excitation itself does not help producing a long-lived signal unless there exists a "regular" long-lived echo for δ-excitation. Then, for soft excitation, the signal created at any moment of time is converted into the echo signal by the propagator in Eq. (14), as it is shown in Fig. 1. Now we can also understand how a single soft pulse with large total flip angle can produce a long-lived signal in a non-linear way (as we explained above, the linear-response signal is zero). The first part of the pulse excites spectral components, while the rest of the pulse acts as a refocusing y-pulse, producing a negative signal. Of course, the excitation with the two-pulse sequence in Fig. 1 is much more efficient.

For $H' = -H$, Eq. (11) describes the echo with complete signal refocusing, and it predicts no echo for $H' = H$. Change of sign of the Hamiltonian (time reversal) can be experimentally realized only for systems with very simple dynamics. The example is the Hahn echo [5] in systems with inhomogeneous spectra. For dipolar-broadened homogeneous spectra, an approximate change of sign can be achieved by using effective Hamiltonians, like in the "magic echo" experiment [6,7]. In practice, the decay time of the "magic echo" can be made an order of magnitude longer than FID. While for coupled many-body systems accurate reversal of a sign of the entire Hamiltonian is a very challenging experimental task, it is much easier to reverse a sign of its part having a simpler structure. Surprisingly, this may create a partial echo, which lives orders of magnitude longer than the "mixing time" of the main Hamiltonian [4].

We will consider the case when H' is close to H, but not equal, and change the notations as $H \to H + \Delta$ and $H' \to H - \Delta$, where Δ is small, compared to H, and does not commute with H. The case $[H, \Delta] = 0$ is not interesting because

$$\exp(L_H\tau)\exp(L_{-\Delta}\tau)\exp(L_H\tau)\exp(L_\Delta\tau) = \exp(L_H\tau)\exp(L_H\tau) = \exp(L_H 2\tau), \quad (15)$$

i.e. the evolution by Δ simply cancels. Even though Δ is small, it is hard to explain the mechanism of the echo by using a perturbation scheme. The reason is that the partial echo of small amplitude is contributed by a small fraction of pairs of states, for which matrix elements of H and Δ are comparable. In the next section, we will introduce a simple three-level model, which can capture some features of the real dynamics. To be more specific, as in Ref. [4], we assume that H is the Hamiltonian of dipole–dipole interactions and Δ is the difference of chemical shifts in the context of solid-state NMR. The pulse sequence implementing this dynamics is the two-pulse Hahn echo sequence [5], which changes the sign of Δ, but does not change the Hamiltonian of dipole–dipole interactions. We will be interested in describing the echo amplitude, decay time, and width.

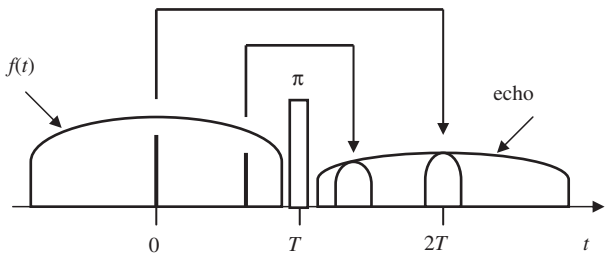

Fig. 1. The echo formed by soft excitation and hard refocusing pulse.

3. Non-selective echo: A three-level model

The smallest number of energy levels, needed to describe the dipolar splitting, is three. At the same time, the three-level model can incorporate the non-commuting operator Δ, which connects the levels with $\Delta m = 0$ (m is the magnetic quantum number), and two single-quantum transitions with $\Delta m = \pm 1$, as follows [4]:

$$H + \Delta = \begin{pmatrix} \omega_d & \Delta & 0 \\ \Delta & -\omega_d & 0 \\ 0 & 0 & 0 \end{pmatrix}, S_X = \begin{pmatrix} 0 & 0 & 1 \\ 0 & 0 & 1 \\ 1 & 1 & 0 \end{pmatrix}, \quad (16)$$

A distribution of dipolar frequencies ω_d will model a "pure" dipolar line shape, without contribution from chemical shift difference. Δ represents the magnitude of the chemical shift difference. For the Hahn sequence $(\pi/2)_Y - \tau - \pi_X$, S_X evolves with the Hamiltonian $H + \Delta$ during the time τ, then, at $t = \tau$, Δ changes the sign.

3.1. The echo amplitude

The problem is solved by diagonalization of the Hamiltonians $H + \Delta$ and $H - \Delta$:

$$U\begin{pmatrix} \omega_d & \Delta & 0 \\ \Delta & -\omega_d & 0 \\ 0 & 0 & 0 \end{pmatrix}U^{-1} = \begin{pmatrix} \lambda & 0 & 0 \\ 0 & -\lambda & 0 \\ 0 & 0 & 0 \end{pmatrix} = D,$$
$$U = \begin{pmatrix} \cos\varphi/2 & \sin\varphi/2 & 0 \\ -\sin\varphi/2 & \cos\varphi/2 & 0 \\ 0 & 0 & 1 \end{pmatrix}, \quad (17)$$

$\tan\varphi = \Delta/\omega_d$, and $\lambda = (\omega_d^2 + \Delta^2)^{1/2}$. $H - \Delta$ is diagonalized by replacing U by U^{-1}, and has the same diagonal form. The signal, x-magnetization, at $t = 2\tau$ can be written as

$$M(2\tau) = Tr(Ue^{iD\tau}U^{-1}S_X Ue^{-iD\tau}U^{-1})(U^{-1}e^{-iD\tau}US_X U^{-1}e^{iD\tau}U)/Tr(S_X^2)$$
$$= (Tr(S_X^2))^{-1}Tr\left\{\begin{pmatrix} 0 & 0 & c(c+s)\phi^- - s(c-s)\phi^+ \\ 0 & 0 & s(c+s)\phi^- + c(c-s)\phi^+ \\ c(c+s)\phi^+ - s(c-s)\phi^- & s(c+s)\phi^+ + c(c-s)\phi^- & 0 \end{pmatrix} \times \begin{pmatrix} s \to -s \\ \phi^+ \to \phi^- \\ \phi^- \to \phi^+ \end{pmatrix}\right\}, \quad (18)$$

where $c = \cos\varphi/2$, $s = \sin\varphi/2$, $\phi^{\pm} = \exp(\pm i\lambda\tau)$, and the second matrix on the last line is obtained from the first matrix by the shown substitutions. By keeping in Eq. (18) only the terms with the phase factors ϕ^+ and ϕ^- compensating each other, after straightforward but lengthy calculations, we can find that the refocused part of magnetization has a very simple form:

$$M_{\text{refocused}}(2\tau) = \sin^2\varphi. \quad (19)$$

If $g(\omega)$ is a normalized distribution function for ω_d, the total echo amplitude can be calculated as

$$M_{\text{echo}}(2\tau) = \int d\omega g(\omega)\sin^2\varphi = \int d\omega g(\omega)(\Delta^2/(\Delta^2+\omega^2)) \approx \pi\Delta g(0) \approx \pi\Delta/\Omega, \quad (20)$$

where Ω is the width of the distribution $g(\omega)$, which models the dipolar line width in our case. When deriving the approximate result in Eq. (20) we assumed that $\Delta \ll \Omega$. The echo amplitude in Eq. (20) is given as a fraction of the equilibrium magnetization, or x-magnetization immediately after the excitation by hard $\pi/2$-pulse.

The above calculations for the three-level system suggest a more general interpretation of the echo as resulting from partial reversal of the dynamic evolution. The echo at $t = 2\tau$ originates from the terms (matrix elements) with compensated phase factors $\phi^{\pm} = \exp(\pm i\lambda\tau)$, where $\pm\lambda$ are eigenvalues of the Hamiltonian (another eigenvalue is zero in our three-level model). Generally,

the phase factors will be $\exp(\pm i\lambda_{ij}\tau)$, where $\lambda_{ij} = \lambda_i - \lambda_j$. After the refocusing pulse at $t = \tau$, matrix elements of S_X which evolved as $\exp(+i\lambda_{ij}\tau)$ acquire fractions of matrix elements with phase factors $\exp(-i\lambda_{ij}\tau)$, which evolved "backward" in time. Subsequent evolution during time τ compensates the phase factors of these fractions and leads to a partial echo.

3.2. The echo decay

A simple three-level model, used to estimate the echo amplitude does not contain a mechanism for the echo decay. In the absence of spin–lattice relaxation, the echo decay results from multi-spin dynamics. (A brief discussion of the role of molecular motions will be given later.) The origin of the very long time scale can be viewed as follows. Both the main Hamiltonian of dipole–dipole interactions H and the observable S_X are invariant under π_X rotation, described by the operator $\pi_X = \exp(i\pi S_X)$. The eigenfunctions of H can be rearranged to become also eigenfunctions of π_X and classified according to their "π_X-parity". Each of the new functions is a linear combination of two eigenfunctions with the same eigenvalue of H and opposite signs of the magnetic quantum number m. S_X has no matrix elements between the functions of different parity and, in the absence of the symmetry-breaking perturbation Δ, its evolution happens independently in the two subspaces of eigenfunctions of H. Total dynamics can be viewed as happening in two fast subsystems with the Hamiltonian H, coupled by the weak interaction Δ. Evolution by Δ leads to a complete mixing and disappearance of any transverse signals. Therefore, we expect that $|\Delta|^{-1}$ may be the longest time scale in our system, and the decrement of the echo decay can be estimated as $|\Delta|$. Such an estimate is not very far from experimental echo decay rates in static solids with infinite network of dipolar couplings. The echo decay rate also determines the limiting line width, which can be achieved by soft excitation in a two-pulse experiment: soft excitation pulse, followed by hard refocusing π-pulse. It is interesting that for unresolved chemical shifts, when their differences are averaged by fast flip-flops, the width of the chemical shift distribution can be estimated from both the echo amplitude and the echo decay rate.

3.3. The echo shape

At this moment, very little is known about the echo width and shape, even though they are important characteristics for practical applications. As an example, the inverse of the echo width determines the range of frequencies where a selective pulse can excite sharp response signals. The height of the response spectrum (i.e. sensitivity) is proportional to the echo width. The three-level model described above would predict the echo width about $|\Delta|^{-1}$, which is very different from experimental observations. The experimental echo widths are much shorter than that. The reason is that the actual structure of the energy levels is more complex. Even though the echo is contributed by pairs of levels with the energy separations about $|\Delta|$ for $\Delta m = 0$, the transitions with $\Delta m = \pm 1$ are not limited to a transition to the state with zero energy. At the same time, since only a small fraction of states participate in the echo formation, and their distribution of energies can be narrower, the echo width may be considerably longer than the conventional FID signal. As an example, in adamantane the echo width is about ten times longer than the free-induction decay signal [4]. Sometimes, like in liquid crystal 5CB (4-Cyano-4′-pentylbiphenyl), the echo width is the same as the decay time of the conventional FID signal. In general, experimentally observed echo shape can be asymmetric, so that the "forward" and "backward" Fourier transforms of its halves produce different spectra. In this respect, the echo is very different from the conventional echo in inhomogeneous systems, where the echo shape reproduces the FID shape. It is also an indication that the density matrix at the center of the echo significantly differs from S_X.

3.4. Molecular motions

Sharp response signals and long-lived echoes are also observed in many soft solids with internal molecular motions and even in viscous liquids. As an example, the echo is observed in soft polymers with non-equivalent protons. In NMR, the effect of molecular motions is usually calculated by using a semi-classical description, when the parameters of the spin Hamiltonian are modulated by random molecular motions:

$$H(t) = H_d(t) + \Delta(t). \tag{21}$$

In the presence of slow molecular motions, with correlation times $\tau_c \sim |H_d|^{-1}$, one would expect that all spin correlations are destroyed at times longer than τ_c. However, there are experimental indications that the echo life time can be much longer than τ_c. A possible explanation can come from fully quantum description of molecular motions [8] using the time-independent total Hamiltonian

$$H = (H_d + F) + \Delta, \tag{22}$$

where F is the Hamiltonian of the lattice. When formulated this way, the problem looks very similar to the one we discussed above. The refocusing π_X pulse does not affect the main Hamiltonian $(H_d + F)$ but changes the sign of Δ. Whether or not the echo may reveal deterministic dynamics of seemingly random molecular motions is yet to be found.

4. Conclusion

We discussed an unusual type of long-lived NMR echo, which can be excited in solids with homogeneously broadened dipolar spectra by a simple two-pulse Hahn sequence $(\pi/2)_Y - \tau - \pi_X$. The echo is formed when there are nuclei with small difference of resonance frequencies (chemical shifts) directly coupled by stronger dipole–dipole interactions. The relative echo amplitude can be estimated as $\pi\Delta/\Omega$, where Ω is the width of the conventional spectrum and Δ is the difference of chemical shifts. The echo decay rate is on the order of Δ. Replacement of the first $(\pi/2)_Y$ pulse, or both the excitation and refocusing hard pulses, by soft pulses allows producing response signals of variable duration and intensity. This capability will be valuable in MRI applications. Development of spectroscopic applications would probably require a more detail study of the echo mechanism.

References

[1] A.K. Khitrin, V.L. Ermakov, B.M. Fung, Information storage using a cluster of dipolar-coupled spins, Chem. Phys. Lett. 360 (2002) 161–166.
[2] A.K. Khitrin, V.L. Ermakov, B.M. Fung, Nuclear magnetic resonance molecular photography, J. Chem. Phys. 117 (2002) 6903–6906.
[3] B.M. Fung, V.L. Ermakov, A.K. Khitrin, Coherent response signals of dipolar-coupled spin systems, Z. Naturforsch 59a (2004) 209–216.
[4] A.K. Khitrin, Selective excitation of homogeneous spectral lines, J. Chem Phys. 134 (2011) 154502.
[5] E. Hahn, Spin Echoes, Phys. Rev. 80 (1950) 580.
[6] W.-K. Rhim, A. Pines, J.S. Waugh, Violation of spin-temperature hypothesis, Phys. Rev. Lett. 25 (1970) 218.
[7] W.-K. Rhim, A. Pines, J.S. Waugh, Time-reversal experiments in dipolar-coupled spin systems, Phys. Rev. B 3 (1971) 684–696.
[8] A. Abragam, Principles of Nuclear Magnetism, Oxford University Press, New York, 1961.